Polarization-Engineered High-Efficiency GaInN Light-Emitting Diodes Optimized by Genetic Algorithm

Dong Yeong Kim
Guan-Bo Lin
Sunyong Hwang
Jun Hyuk Park
David Meyaard
E. Fred Schubert, Fellow, IEEE
Han-Youl Ryu
Jong Kyu Kim
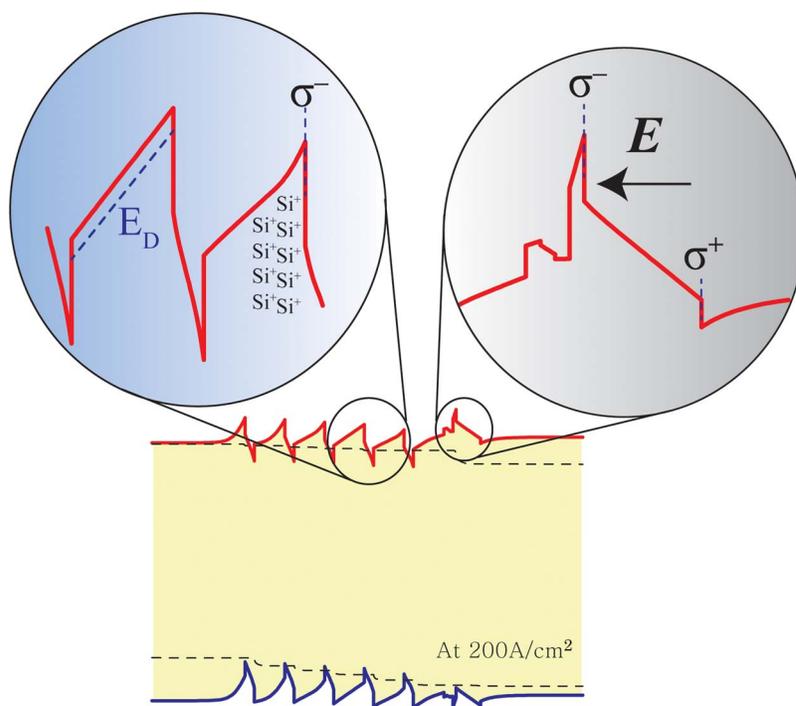
Polarization-Engineered High-Efficiency GaInN Light-Emitting Diodes Optimized by Genetic Algorithm

Dong Yeong Kim,[1] **Guan-Bo Lin,**[2] **Sunyong Hwang,**[1] **Jun Hyuk Park,**[1]
David Meyaard,[2] **E. Fred Schubert,**[2] *Fellow, IEEE*,
Han-Youl Ryu,[3] **and Jong Kyu Kim**[1]

[1]Department of Materials Science and Engineering, Pohang University of Science and Technology,
Pohang 790-784, Korea
[2]Future Chips Constellation, Department of Electrical, Computer, and Systems Engineering,
Rensselaer Polytechnic Institute, Troy, NY 12180 USA
[3]Department of Physics, Inha University, Incheon 402-751, Korea

Abstract: A genetic algorithm is employed to find an optimum epitaxial structure of multiple quantum wells (MQWs) and electron-blocking layer (EBL) for a GaInN-based light-emitting diode (LED). The optimized LED is composed of locally Si-doped quantum barriers (QBs) in the MQWs and a quaternary heterostructured AlGaInN EBL having a polarization-induced electric field directed oppositely to that of a conventional AlGaN EBL. The optimized LED shows 15.6% higher internal quantum efficiency, 24.6% smaller efficiency droop, and 0.21 V lower forward voltage at 200 A/cm^2 comparing to the reference LED, which has fully Si-doped QB and 20-nm-thick Al$_{0.19}$Ga$_{0.81}$N EBL. We find that local Si doping near the QB/QW interface compensates the negative polarization-induced sheet charge at the interface and reduces electric field in the QWs, thereby enhancing electron–hole wave function overlap. In addition, the inverted polarization field in the quaternary EBL provides a high barrier for electrons but a low barrier for holes, resulting in enhanced electron-blocking and hole-injection characteristics.

Index Terms: Light-emitting diodes, genetic algorithm, polarization engineering.

1. Introduction

Optimization of the epitaxial structure of GaN-based light-emitting diodes (LEDs) with high efficiency and reduced efficiency droop has been one of the hottest research topics for highly efficient white LEDs used for general illumination applications. In particular, finding optimum epitaxial structures for the multiple-quantum well (MQW) active region and electron blocking layer (EBL) is important because they have a strong influence on the injection and the radiative recombination of carriers, both of which are directly related to the LED performance [1]–[10].

Various MQW and EBL structures have been proposed and demonstrated to enhance device performance including saw-like quantum well (QW) [1], [2], lattice matched AlInN quantum barriers (QBs) [3] and EBLs [4], polarization-matched AlGaInN QBs [5], [6] and EBLs [6], [7], Al composition graded AlGaN based EBL [8], and AlGaN/GaN superlattice EBL [9], [10]. However, it is extremely difficult to find a truly optimized epitaxial design of GaN-based LEDs through case studies, iterative methods, or trial-and-error experiments due to following reasons. First, there are simply too many structural parameters including layer thickness, alloy composition, doping concentration, and the composition and doping profile in each of the epitaxial layers constituting the complex heterostructure LED. Second, structural parameters mutually influence each other, resulting in an enormous parameter space which, in its entirety, represents all possible combinations of variables. Third, performance criteria such as internal quantum efficiency (IQE), magnitude of efficiency droop, and forward voltage are inextricably coupled, which makes the optimization process even more complex, and calls for the development of a new performance criterion (fitness function) to assess the performance.

A promising method for overcoming these difficulties in LED optimization is the genetic algorithm (GA) which adopts an artificial evolutionary process that is ruled by the law of survival of the fittest and includes a fitness function, selection criteria, and reproduction by cross-over, mutation and random generation [11], [12]. In the GA optimization process, LEDs with superior characteristics (as assessed by a predetermined performance criterion, i.e., the fitness function), are selected to survive the *selection* process. Based on the fitness function, a fitness value is determined for each LED structure of the population. The fitness value allows us to rank-order the entire LED population and perform the selection process. Then, the structural parameters of the subsequent-generation LEDs are generated by the *reproduction* process that includes cross-over between randomly selected LEDs, mutation, i.e., random changes in parameters, and random generation of new LEDs. This process allows one to avoid getting stuck in *local* performance maxima (rather than finding the *global* performance maximum). The iterative selection and reproduction processes make the GA very suitable for dealing with optimization of complex systems having a huge number of cross-coupled variables (like LEDs). Recently, Zhu *et al.* [12], based on the use of a GA optimization process, proposed the use of undoped QBs and a multilayer EBL to enhance the performance of an LED. However, the forward voltage and important structural parameters such as the thickness and Mg doping of the EBL, the Si doping profile of the QBs, and their mutual influence were not considered in their optimization.

In the present study, we employ a GA to find a truly optimized epitaxial structure of GaN-based QBs and an AlGaInN-based EBL constituting GaInN-based blue LEDs. Multiple structural parameters are simultaneously optimized including the Si doping profile in the QBs, the Al and In composition in the EBL, and the Mg doping profile and total thickness of EBL. In addition, the forward voltage is considered in the fitness function as well as the IQE and the degree of the efficiency droop. As a result, an optimized LED is obtained that has a smaller forward voltage as well as an overall high IQE with reduced efficiency droop. For understanding its enhanced performance, the optimized LED was further numerically investigated using an in-house self-consistent device simulator, PYSDS (PYthon Semiconductor Device Simulator). We found that an optimized Si doping profile can enhance the radiative recombination probability by screening the polarization-induced electric field in the QWs and the optimized hetero-structured AlGaInN EBL can improve the hole injection efficiency as well as electron-blocking efficiency due to the inverted polarization-induced electric field direction as compared to a conventional AlGaN EBL.

2. LED Optimization by Genetic Algorithm

The reference LED structure as the starting structure for the optimization is schematically shown in Fig. 1(a). The reference LED consists of a 200 nm-thick n-type GaN cladding layer (Si doping concentration of 7×10^{18} cm^{-3}), a five-period MQW with 3 nm-thick undoped Ga$_{0.85}$In$_{0.15}$N wells and 10 nm-thick Si-doped GaN barriers (Si doping concentration of 5×10^{18} cm^{-3}), a 6 nm-thick undoped-GaN spacer layer, a 4 nm-thick Mg-doped GaN hole-injection layer (Mg doping:
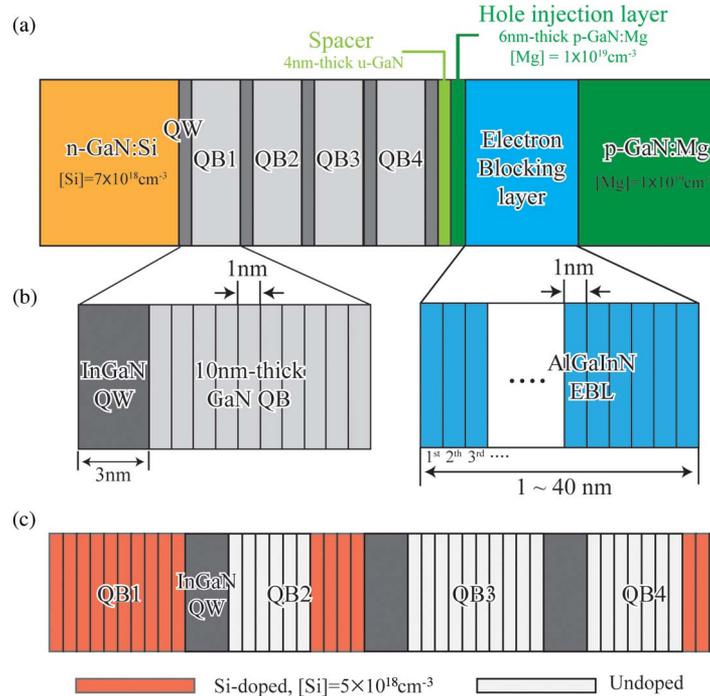
Fig. 1. (a) LED structure used in optimization. (b) For the GA optimization, the QBs and EBL are decomposed into 1 nm-thick sub-layers. (c) Optimization results for the Si doping in the QBs. Red sub-QBs are doped with Si of 5×10^{18} cm^{-3} and gray sub-QBs are undoped.

1×10^{19} cm^{-3}), an 20 nm-thick Mg-doped Al$_{0.19}$Ga$_{0.81}$N EBL (Mg doping: 1×10^{19} cm^{-3}), and a 200 nm-thick p-type Mg-doped GaN cladding layer (Mg doping concentration of 1×10^{19} cm^{-3}). Fully Si-doped QBs in the MQW active region and bulk AlGaN EBL are widely adopted to provide enough free electrons to QWs facilitating carrier transport, and to suppress electron overflow, respectively, which is the reason why such particular structure is chosen for the reference in the GA optimization.

Here, QBs and AlGaInN EBL (instead of AlGaN EBL) are simultaneously optimized. Both QBs and EBL are decomposed into 1 nm-thick sub-layers to optimize the profile of doping and alloy composition, as shown in Fig. 1(b). The allowed range of the Si doping concentration is from 0 to 5×10^{18} cm^{-3} for each sub-QB layer. For the EBL, we optimized Al and In composition, Mg concentration of each sub-EBL layer and total thickness of the EBL from 1 nm to 40 nm. The allowed range of both Al and In compositions and Mg doping concentration of EBL sub-layers are set from 0 to 0.30, and from 0 to 1×10^{19} cm^{-3}, respectively, in consideration of experimentally achievable values using typical growth conditions of metal-organic vapor phase epitaxy.

Next, the overall process of the GA-based LED optimization is described. At first, a large number of different LED structures, in this study 1500 LED structures, with different structural parameters as described above, are randomly generated and evaluated in terms of the fitness function defined as

$$\text{Fitness value} = \frac{[\text{IQE}_{\text{peak}} + \text{IQE@200 A} \cdot \text{cm}^{-2}] - \text{Efficiency droop}}{V_F}$$

where IQE$_{\text{peak}}$ is the peak IQE value, V_F is the forward voltage at 200 A/cm^2, and the efficiency droop defined as

$$\text{Efficiency droop} = \frac{\text{IQE}_{\text{peak}} - \text{IQE@200 A/cm}^{-2}}{\text{IQE}_{\text{peak}}}$$

TABLE 1

Al and In composition, and Mg doping concentration of the twelve sub-layers of the 12 nm-thick optimized EBL. The ordinal numbers from 1st to 12th indicate the position of the sub-EBL layers such that 1st sub-layer is grown after the hole-injection layer and 12th sub-layer is the last-grown layer, as shown in Fig 1(b).

	1st	2nd	3rd	4th	5th	6th	7th	8th	9th	10th	11th	12th
Al	0.22	0.27	0.2	0.3	0.3	0.3	0.3	0.3	0.3	0.3	0.3	0.3
In	0.09	0.13	0.09	0.05	0.15	0.15	0.15	0.15	0.15	0.15	0.15	0.15
[Mg]	$1 \times 10^{19} cm^{-3}$ (Maximum value)											

IQE in this calculation is defined as

$$IQE(N) = \frac{R_{sp}(N)}{R_{sp}(N) + R_{SRH}(N) + R_{Auger}(N) + J_{leakage}/e}$$

where $R_{sp}(N)$, $R_{SRH}(N)$, $R_{Auger}(N)$ are spontaneous radiative recombination rate, Shockley-Read-Hall (SRH) recombination rate, and Auger recombination rate as a function of carrier, N, respectively, $J_{leakage}$ is electron overflow current density, and e is the element charge. Influence of photon recycling including optical absorption and re-emission processes which can affect the IQE [13] is not considered in the fitness value calculation.

Using the fitness function, a fitness value can be calculated for each LED structure of the population. IQE and forward voltage of all LEDs are calculated by PYSDS that solves the Poisson equation and a drift-diffusion model self-consistently. Material and band parameters used in this calculation can be found in [14] and [15], respectively. After the determination of the fitness value, the top-10% performing LEDs are made to survive the selection process. The other 90% of the LEDs are replaced with newly created LEDs in the reproduction process: 60% LEDs are the offspring of the surviving LEDs created by structural crossover, 20% LEDs are the mutations of the survivors, and 10% LEDs are randomly generated ones. All these LEDs compose a new population of LEDs, called the next generation, and they are evaluated, selected, and reproduced again in an iterative process. The population evolves to have an increasingly higher fitness value, thus, a higher efficiency, reduced efficiency droop, and a smaller forward voltage. Eventually, the fitness value of the best LED in a generation becomes saturated and doesn't change anymore. In this optimization, the highest fitness value doesn't change for more than 400 generations and we adopted the value as the optimum. Optimized Si doping concentration in each QB is visualized by color in Fig. 1(c). Red and gray QB sub-layers indicate a Si-doped region with concentration of 5×10^{18} cm^{-3} and an undoped region, respectively. The first QB is Si-doped whereas the third QB is not doped. Interestingly, the QB2 and QB4 are locally doped near the QB/QW interface.

Structural parameters of the optimized AlGaInN EBL are shown in Table 1 including the Al and In compositions, and the Mg doping concentration. The optimized quaternary EBL consists of twelve 1 nm-thick sub-layers, i.e., total thickness of 12 nm, all of which are Mg doped with the highest allowed concentration of 1×10^{19} cm^{-3}. This indicates that a highly p-doped EBL is preferred for enhanced hole-injection over a reduced hole-energy barrier into the active region [16]. The combination of Al and In compositions in each sub-layer varies intricately for the first four sub-layers, and becomes fixed to $Al_{0.3}Ga_{0.55}In_{0.15}N$ for the remaining eight sub-layers. Note that a huge energy barrier for electrons is expected at the 4th sub-layer $Al_{0.3}Ga_{0.65}In_{0.05}N$ (see also Fig. 4, to be discussed below).

3. Discussion

Device characteristics of the optimized LED is numerically investigated and compared with the reference LED having fully Si-doped QBs (Si doping concentration of 5×10^{18} cm^{-3}), and a
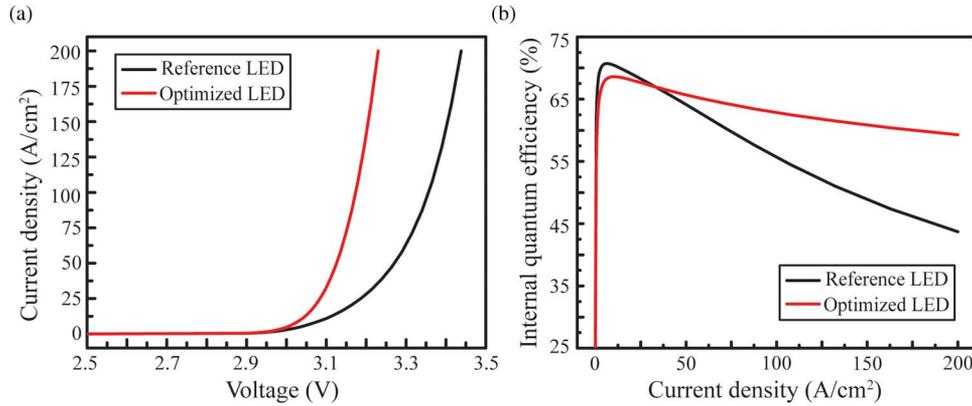
Fig. 2. (a) J-V characteristics and (b) internal-quantum-efficiency-versus-current-density curves of the reference LED and the GA-optimized LED.

20 nm-thick Mg-doped $Al_{0.19}Ga_{0.81}N$ EBL (Mg doping concentration: 1×10^{19} cm^{-3}). Fig. 2(a) and (b) shows the current-density-versus-voltage (J-V) characteristics and the IQE-versus-current-density curves of the reference and the optimized LED. Forward voltage of the optimized LED is 3.23 V at injection current of 200 A/cm^2 which is 0.21 V lower than that of the reference [Fig. 2(a)]. In addition, the optimized LED shows higher IQE at 200 A/cm^2 (59.3% for the optimized LED and 43.7% for the reference) although its peak IQE is slightly lower than for the reference LED. Furthermore, the optimized LED has a significantly reduced efficiency droop (13.6% for the optimized LED and 38.2% for the reference).

In order to understand effect of the optimized Si doping profile on LED performance, the conduction band (CB) profile of the reference and the optimized LED are compared. Fig. 3(a) shows CB profiles near MQWs for both LEDs at the injection current density of 200 A/cm^2. The CB profiles have different slopes in the QWs indicating different electric field in QWs. This is a critical factor making a difference in radiative recombination probability [17]. The electric field distribution in the QWs, calculated by the equation

$$\boldsymbol{E} = -\frac{1}{e}\frac{dE_C}{dx} \ [V/m]$$

where, e is the elementary charge, E_C is the conduction band energy, is shown in Fig. 3(b). The optimized LED has smaller electric field inside the QWs than the reference LED, which enhances the radiative recombination probability by reducing spatial separation of electron and hole wave functions.

The reduced electric field in the optimized MQWs is attributed to polarization-field screening by the locally doped Si dopants. After ionization, the fixed positive Si ions (Si^+) can compensate the negative polarization sheet charge at the QB/QW interface (i.e., the first-grown interface of the QW). For the locally-doped QBs obtained from the optimization, the estimated surface density of ionized Si is the order of 10^{12} e/cm^2 which is same order of magnitude with polarization charge density between $Ga_{0.85}In_{0.15}N$ QW and GaN QB ($\sim10^{12}$ e/cm^2). Conversely, such Si^+ can intensify the effect of the positive polarization sheet charge at the QW/QB interface (i.e., the second-grown interface of the QW). Therefore, Si doping only occurs locally near the QB/QW interface so that the QB2 and QB4 in the optimized LED effectively reduce the polarization-induced electric field and enhance the radiative recombination rate.

An interesting point is that the amount of free electrons provided by the locally doped QBs is comparable to the fully doped QBs despite fewer Si donors; this is due to incomplete ionization. Degree of donor ionization is expressed as

$$\frac{N_D^+}{N_D} = \frac{1}{1 + g \cdot \exp[-(E_D - F_N)]} = \frac{1}{1 + g \cdot \exp[-(E_C - E_{ion} - F_N)]}$$
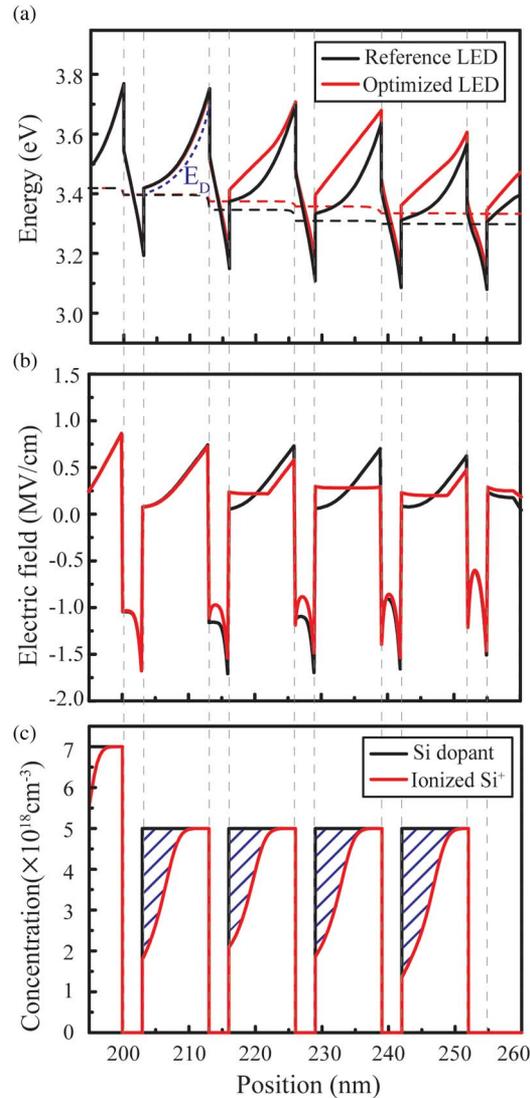
Fig. 3. (a) Conduction band diagram and (b) electric field distribution in the reference LED and the optimized LED at injection current level of 200 A/cm². The dashed line in the second QB of (a) indicates donor level, E_D. (c) Si and ionized Si dopant concentrations of the reference LED. Dashed region indicates concentration of un-ionized Si donors.

where, N_D is the concentration of the donors, N_D^+ is the concentration of ionized donors, g is the degeneracy which is 2 for donors, E_D is the donor energy level, and F_N is the quasi Fermi level for electrons under the operation condition [18]. Here, E_D can also be expressed as $E_C - E_{ion}$, where E_C is the conduction band energy and E_{ion} is the donor ionization energy. The ionization energy is a constant and the quasi-Fermi level remains almost same in each QB as shown in Fig. 3(a). Therefore, donors near QW/QB interface are incompletely ionized due to small energy difference between F_N and E_D whereas almost all donors near QB/QW interface are ionized. Fig. 3(c) shows the concentration profiles of Si dopant and ionized Si dopant in QBs of the reference LED, clearly indicating incomplete ionization near QW/QB interfaces as discussed. Locally Si doped QBs can provide enough ionized donors and free electrons to effectively screen the polarization charges.

A remaining question is why the QB2 and QB4 are locally doped and the other QBs are not. A possible explanation may be obtained from the standpoint of carrier transport. The relative
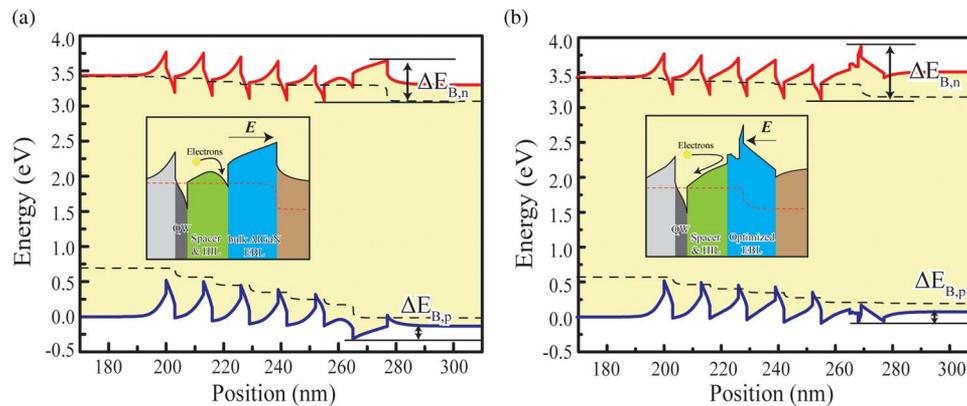
Fig. 4. Energy band diagram of (a) the reference LED and (b) the optimized LED at 200 A/cm^2. Effective energy barrier for electrons, $\Delta E_{B,n}$, and holes, $\Delta E_{B,p}$, are indicated in both figures. Inset: Conduction band diagrams near EBL region and electric field direction inside EBL.

energy level (E_C) of adjacent QB layers can be tuned by adjusting the doping state of each layer. In the case of an NN junction (or PP junction), the more highly doped layer has the lower (higher) energy level for the respective carrier. Therefore, QBs near the n-GaN are preferred to be highly n-doped to improve the electron transport by lowering the energy barrier for electrons. On the other hand, undoped QBs (even p-doped) near the p-GaN are preferred to raise the electron energy level (i.e., E_C) which makes hole transport easier [19]. The optimized QBs basically follow the concept that the QB1 is fully doped and the QB3 is undoped. It is our understanding that the locally Si-doped QBs are for reducing the electric field. We cannot yet offer an explanation as to why the only QB2 and QB4 are locally doped. However, this, paradoxically, shows the strength of the GA-based optimization in that the GA can lead us to advanced structures that would be difficult to design by conventional methods.

In order to investigate the effects of the optimized AlGaInN EBL on its electron blocking and hole injection properties, the effective energy barriers for electrons and holes are calculated from the energy band diagram under operation conditions (drive current density of 200 A/cm^2). The energy band diagrams of the reference and optimized LED are shown in Fig. 4. The effective energy barrier for electrons, $\Delta E_{B,n}$, is defined as difference between highest E_C energy level of the EBL and lowest E_C energy level of QWs, and similarly, for holes, $\Delta E_{B,p}$ is defined as difference between lowest E_V energy level of the EBL and the E_V energy level of p-GaN bulk region, as indicated in the figure. $\Delta E_{B,n}$ of the reference and the optimized LED are 0.569 eV and 0.760 eV, respectively. Thus, the optimized EBL can more effectively suppress the electron leakage from the MQWs compared to the reference. In addition, the optimized EBL is expected to show the better hole injection efficiency because $\Delta E_{B,p}$ of the optimized EBL, 0.161 eV, is smaller than that of the reference, 0.187 eV.

Such enhanced properties of the optimized EBL are attributed to the inverted direction of the polarization-induced electric field in the EBL, as shown in the insets of Fig. 4. When employing an AlGaN EBL, a positive sheet charge occurs at the interface of the hole-injection layer and EBL and it pulls down the energy band forming a local hole energy barrier (in the VB) and a local electron potential well (in the CB) that attracts electrons [inset of Fig. 4(a)] [16]. In contrast, the energy band is raised up due to the reverse polarization-induced electric field in the optimized AlGaInN EBL, generating an effective electron-energy barrier and reducing hole-injection energy barrier [inset of Fig. 4(b)]. The inverted polarization-field in the optimized EBL originates from the 4th sub-layer which has wider bandgap energy compared to the other sub-layers. Thus, the 4th sub-layer plays an essential role in enhancing EBL performance by not only suppressing electron overflow enabled by the huge energy barrier but also by generating an inverted polarization-field in the EBL. Recently, the concept of the polarization-inverted EBL structure was proposed in a paper by D. S. Meyaard *et al.* [20] In the paper, it was proposed
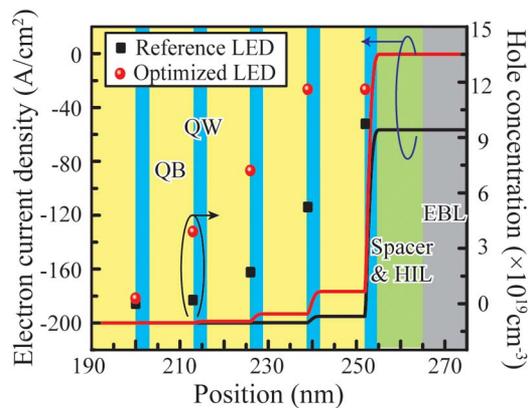
Fig. 5. Electron current density and hole concentration in the reference LED and the GA-optimized LED. HIL stands for hole-injection layer.

that the p-type region including p-cladding layer, EBL, and spacer and remaining LED structures be grown separately and two structures were to be combined through a wafer or chip bonding process to obtain a polarization-inverted EBL. In the present GA optimization, polarization-inverted EBL was also obtained by simply adjusting the alloy composition in a single c-plane epitaxial growth process.

Fig. 5 shows the electron current density and hole concentrations in the QWs of the reference and the optimized LED at the injection current density of 200 A/cm^2. Electron leakage which is denoted by electron current density in the p-type region is significantly suppressed in the optimized LED, indicating enhanced electron-blocking efficiency by the optimized EBL. In addition, the optimized LED shows higher hole concentrations in the QWs than the reference device, which indicates better hole-injection into the active region. These results are consistent with the expectations based on the energy band structure of the optimized EBL, as discussed above.

4. Conclusion

In summary, the epitaxial structure of a GaN-based LED is optimized using a GA which is an algorithm implementing an artificial evolutionary process based on selection and reproduction. The parameters optimized by the GA are the Si doping profile of the locally Si-doped QBs in the MQW active region and the AlGaInN multilayer heterostructure EBL. The overall efficiency (i.e., the peak efficiency and the high-current efficiency), the magnitude of the droop, as well as the forward voltage were taken into account in the fitness function. By taking advantage of the GA, multiple structural variables—including the Si doping profile in the QBs of the MQW active region, the Al and In compositions in the EBL, and the Mg doping concentration and profiles in the EBL—were optimized simultaneously so as to find a truly optimized epitaxial structure. The optimized LED consists of locally Si-doped QBs near the QB/QW interface and an AlGaInN EBL having inverted polarization-field direction compared to the conventional AlGaN EBL. We found that the negative polarization-induced sheet charge at the QB/QW interface is compensated by locally doped Si dopants, so that the electric field in the QWs is reduced and the electron–hole wave function overlap is enhanced and, along with it, the radiative recombination rate. In addition, polarization-field inverted AlGaInN EBL has a higher effective energy barrier for electrons and lower energy barrier for holes than the conventional AlGaN EBL, thereby improving electron-blocking and hole-injection. As a result, the optimized LED has 15.6% higher internal quantum efficiency, 24.6% smaller efficiency droop, and 0.21 V lower forward voltage at 200 A/cm^2 comparing to the reference LED, as desired. This work clearly shows that GA-based LED optimization has great potential to provide solutions that satisfy the strong demand for an LED design that enables high efficiency LED.

References

[1] S.-H. Park, "Radiative efficiency enhancement in blue saw-like InGaN/GaN light-emitting diodes," *Appl. Phys. Exp.*, vol. 6, no. 5, 2013, Art. ID. 052101.

[2] M.-C. Tsai, S.-H. Yen, and Y.-K. Kuo, "Investigation of blue InGaN light-emitting diodes with step-like quantum well," *Appl. Phys. A*, vol. 104, no. 2, pp. 621–626, Aug. 2011.

[3] H. Zhao, G. Liu, R. A. Arif, and N. Tansu, "Current injection efficiency induced efficiency-droop in InGaN quantum well light-emitting diodes," *Solid-State Electron.*, vol. 54, no. 10, pp. 1119–1124, Oct. 2010.

[4] S. Choi *et al.*, "Improvement of peak quantum efficiency and efficiency droop in III-nitride visible light-emitting diodes with an InAlN electron-blocking layer," *Appl. Phys. Lett.*, vol. 96, no. 22, 2010, Art. ID. 221105.

[5] M.-H. Kim *et al.*, "Origin of efficiency droop in GaN-based light-emitting diodes," *Appl. Phys. Lett.*, vol. 91, no. 18, 2007, Art. ID. 183507.

[6] M. F. Schubert *et al.*, "Polarization-matched GaInN/AlGaInN multi-quantum-well light-emitting diodes with reduced efficiency droop," *Appl. Phys. Lett.*, vol. 93, no. 4, 2008, Art. ID. 0411102.

[7] Y.-K. Kuo, M.-C. Tsai, and S.-H. Yen, "Numerical simulation of blue InGaN light-emitting diodes with polarization-matched AlGaInN electron-blocking layer and barrier layer," *Opt. Commun.*, vol. 282, no. 21, pp. 4252–4255, Nov. 2009.

[8] C. H. Wang *et al.*, "Hole injection and efficiency droop improvement in InGaN/GaN light-emitting diodes by band-engineered electron blocking layer," *Appl. Phys. Lett.*, vol. 97, no. 26, 2010, Art. ID. 261103.

[9] Y. Y. Zhang and Y. A. Yin, "Performance enhancement of blue light-emitting diodes with a special designed AlGaN/GaN superlattice electron-blocking layer," *Appl. Phys. Lett.*, vol. 99, no. 22, 2011, Art. ID. 221103.

[10] J. H. Park *et al.*, "Enhanced overall efficiency of GaInN-based light-emitting diodes with reduced efficiency droop by Al-composition-graded AlGaN/GaN superlattice electron blocking layer," *Appl. Phys. Lett.*, vol. 103, no. 6, 2013, Art. ID. 061104.

[11] R. L. Haupt and S. E. Haupt, *Practical Genetic Algorithms*, 2nd ed.   New York, NY, USA: Wiley, 2004.

[12] D. Zhu *et al.*, "Genetic algorithm for innovative device designs in high-efficiency III–V nitride light-emitting diodes," *Appl. Phys. Exp.*, vol. 5, no. 1, 2012, Art. ID. 012102.

[13] J.-B. Wang, S. R. Johnson, D. Ding, S.-Q. Yu, and Y.-H. Zhang, "Influence of photon recycling on semiconductor luminescence refrigeration," *J. Appl. Phys.*, vol. 100, no. 4, 2006, Art. ID. 043502.

[14] J. Piprek, *Nitride Semiconductor Devices: Principles and Simulation*.   Weinheim, Germany: Wiley, 2007.

[15] I. Vurgaftman and J. R. Meyer, "Band parameters for nitrogen-containing semiconductors," *J. Appl. Phys.*, vol. 94, no. 6, 2003, Art. ID. 3675.

[16] E. F. Schubert, *Light-Emitting Diodes*, 2nd ed.   Cambridge, U.K.: Cambridge Univ. Press, 2006.

[17] G.-B. Lin *et al.*, "Effect of quantum barrier thickness in the multiple-quantum-well active region of GaInN/GaN light-emitting diodes," *IEEE Photon. J.*, vol. 5, no. 4, 2013, Art. ID. 1600207.

[18] G. Xiao, L. Lee, J. J. Liou, and A. Ortiz-Conde, "Incomplete ionization in a semiconductor and its implications to device modeling," *Microelectron. Rel.*, vol. 39, no. 8, pp. 1299–1303, Aug. 1999.

[19] D. Zhu *et al.*, "Enhanced electron capture and symmetrized carrier distribution in GaInN light-emitting diodes having tailored barrier doping," *Appl. Phys. Lett.*, vol. 96, no. 12, 2010, Art. ID. 121110.

[20] D. S. Meyaard, *et al.*, "GaInN light-emitting diodes using separate epitaxial growth for the p-type region to attain polarization-inverted electron-blocking layer, reduced electron leakage, and improved hole injection," *Appl. Phys. Lett.*, vol. 103, no. 20, 2013, Art. ID. 201112.